Applied Geochemistry 125 (2021) 104824

Contents lists available at ScienceDirect

Applied Geochemistry

journal homepage: http://www.elsevier.com/locate/apgeochem

Suitability of calibrated X-ray fluorescence core scanning for environmental geochemical characterisation of heterogeneous sediment cores

Tatiana Goldberg [a,e,*], Rick Hennekam [b], Laura Wasch [a], Gert-Jan Reichart [b,c], Oliver Rach [e], Jessica A. Stammeier [e], Jasper Griffioen [a,d]

[a] TNO Geological Survey of the Netherlands, Princetonlaan 6, 3584 CB, Utrecht, the Netherlands
[b] NIOZ Royal Netherlands Institute for Sea Research, Department of Ocean Systems, And Utrecht University, P.O. Box 59, 1790 AB, Den Burg, Texel, the Netherlands
[c] Department of Earth Sciences, Faculty of Geosciences, Utrecht University, P.O. Box 80.121, 3508 TA, Utrecht, the Netherlands
[d] Copernicus Institute of Sustainable Development, Faculty of Geosciences, Utrecht University, P.O. Box 80.115, 3508 TC, Utrecht, the Netherlands
[e] GFZ - German Research Centre for Geosciences, Telegrafenberg, D-14473, Potsdam, Germany

ARTICLE INFO

Editorial handling by Prof. M. Kersten

Keywords:
Core scan
Multivariate log-ratio calibration
Geochemistry
Element contents
Mineralogy
Diagenesis

ABSTRACT

Multi-element analysis of discrete samples via X-Ray fluorescence or inductively coupled plasma spectrometry is commonly used to characterise the composition of solid geo-materials for environmental geochemical characterisation. Conventional geochemical analysis of individual samples is time consuming and costly, which often results in low-resolution sampling with the danger of missing crucial information. X-ray fluorescence Core Scanning (XCS) provides an alternative method to obtain elemental information, which can be potentially used quantitatively when combined with the Multivariate Log-ratio Calibration (MLC) approach. The suitability of the XCS-MLC method was tested for environmental geochemical characterisation on four terrestrial Holocene-Pleistocene sediment cores that have a variable lithology (clay, sand, peat, with variable calcareous content), were stored at ambient room conditions and scanned post sampling. Element contents based on XCS-MLC and conventional geochemical analysis proved to be comparable ($R^2 > 0.5$) for Al, Ca, Cr, Fe, K, Sr, Mn, Ni, Pb, Rb, S, Si, Ti, Zn, Zr, and also for Br as proxy for organic matter. For As, Cu and Ba the correlations were less satisfactory ($R^2 < 0.4$) partially due to the low concentration ranges present in these sediments. For some samples aberrant high values for Ca, Fe, S, and Zn were introduced by application of the MLC method due to extrapolation outside the MLC-calibrated range. Similar to the conventional element analyses the XCS-MLC approach has the ability to retrieve quantitative element contents and enable the calculation of mineral phases such as calcium carbonate and reactive iron species. Both conventional and XCS-MLC methods reproduced the average contents per sediment layer and mostly their ranges. Nevertheless, local features such as diagenetic enrichments were not always evident from the discrete samples. Thus, a better understanding of the spatial heterogeneity in geochemical and mineralogical contents within the sediment layers was obtained with the additional XCS-MLC data. Our study shows that also cores stored under unfavourable conditions can be reliably re-analysed with XCS to generate high resolution records.

1. Introduction

Environmental geochemical characterisation of sediments, soils and rocks is performed, among other, to, 1) recognise background composition and the natural range of variation (Tebbens et al., 2000; Amorosi et al., 2007; Salonen and Korkka-Niemi, 2007; Reimann et al., 2018), 2) acknowledge anthropogenic pollution and impact of land use (Koelmans, 1998; Davide et al., 2003; Sterckemann et al., 2004; Reimann and Garret, 2005; Van Gaans et al., 2007; Singh et al., 2008; Acosta et al., 2011; Saaltink et al., 2014), 3) characterise the buffering capacity for inflowing pollutants (Rodrigues et al., 2010; Van Gaans et al., 2011; Griffioen et al., 2012), and 4) predict the geochemical behaviour upon implementation of technologies such as soil and groundwater remediation, managed aquifer recharge, underground thermal energy storage and eco-engineering (Griffioen and Appelo, 1993; Prommer and Stuyfzand, 2005; Doulati Ardejani et al., 2011; Wanner et al., 2012; Anawar, 2015; Pedersen et al., 2015; Saaltink et al., 2016; Pit et al., 2017).

For these purposes, multi-element geochemical analysis is used on a

* Corresponding author. GFZ - German Research Centre for Geosciences, Telegrafenberg, D-14473, Potsdam, Germany
E-mail address: goldberg@gfz-potsdam.de (T. Goldberg).

https://doi.org/10.1016/j.apgeochem.2020.104824
Received 19 March 2020; Received in revised form 2 October 2020; Accepted 8 November 2020
Available online 18 November 2020

routine basis to characterise the composition of solid geo-materials. The methodology is typically based on discrete samples that are manually collected from drilling cores, dug pits, grab samplers, quarry walls, etc. In some cases, samples from a similar geo-scientific unit may be mixed prior to analysis to composite samples in order to have better spatial representativeness. The latter is, for example, done in soil monitoring where samples from the same soil horizon out of an agricultural field are mixed prior to analysis. Van Gaans et al. (2011) and Griffioen et al. (2012) established and tested a methodology to characterise sedimentary formations in the shallow subsurface (<30–35 m depth) for environmental geochemical purposes. They found that knowledge of lithological and lithostratigraphical stratification is necessary at the regional scale because the reaction capacity is also partially controlled by post-depositional diagenesis and palaeohydrology. It was found that 45 samples per stratum is sufficient in most instances. The established methodology provides regional statistics on central tendency (mean, median) and variability (variance, interpercentile ranges) irrespective of regional geostatistical patterns and borehole-scale variability.

The geochemical analysis of individual samples is time consuming and costly. An alternative approach is the use of X-ray fluorescence Core Scanning (XCS) to obtain multi-element geochemical data from sediment cores (Jansen et al., 1998). The core scanner scans along the surface of a natural sample and only requires minimal preparation beforehand compared to conventional XRF analysis on pre-prepared fused beads or pressed powder pellets. The XRF-scanning instruments are generally equipped with holders to fit sediment cores (typically to 1.5 m in length) but can also hold smaller sized samples. The XCS method measures such samples non-destructively, preserving sample material for additional destructive analyses. Moreover, the XCS is known to be relatively fast, high-resolution (cm to mm sampling intervals), and per measurement comparably low-cost (Richter et al., 2006; Croudace and Rothwell, 2015). Borehole-scale variability may thus be better assessed using XCS. However, raw XCS intensities do not readily translate to element quantities (Weltje and Tjallingii 2008), which are of prime interest for environmental geochemical purposes. Previous attempts to achieve element contents by means of direct linear calibration and univariate log-ratio calibration did not deliver satisfactory results and only allowed for element ratios to be considered (Jansen et al., 1998; Croudace et al., 2006; Tjallingii et al., 2007; Weltje and Tjallingii 2008). More recently, the superior Multivariate Log-ratio Calibration (MLC) method was proposed, calibrating all elements simultaneously using centred log ratios (Weltje et al., 2015). The MLC approach minimises the uncertainty on predicted elemental quantities by accommodating for adsorption and enhancement effects (i.e., matrix effects) on intensities and allows to determine absolute concentrations (Weltje et al., 2015). The MLC calibration has been successfully applied in paleoenvironmental and paleoceanographic studies (e.g., Grant et al., 2017; Falster et al., 2018; Gregory et al., 2019; Hennekam et al., 2019) and has recently also been applied in an environmental geochemical assessment (Lee et al., 2019). Absolute element contents rather than element ratios or intensities are of primary interest for environmental assessments. This is due to element contents being frequently utilised to infer the mineralogical composition of a sediment (e.g., Cox et al., 1995; Von Eynatten et al., 2003; Yan et al., 2009; Van Gaans et al., 2011; Griffioen et al., 2012). Iron, Ca and Al contents may be used to calculate reactive iron and calcium carbonate contents. Total reactive iron (FeTR) is Fe bound in Fe-(oxyhydr)oxide, carbonate, sulphide and phosphate and also sorbed Fe (Poulton and Raiswell, 2002). Total reactive Fe can be calculated by deduction of non-reactive Fe from the total Fe content (Huisman and Kiden, 1998; Dellwig et al., 2002; Griffioen et al., 2012; see Chapter 2.3). Comparably, Ca carbonate can be calculated from the Ca content where the distinction is made between silicate-bound Ca (in particular as Ca feldspar) and carbonates (Bakker et al., 2007; Griffioen et al., 2012, see Chapter 2.3).

The objective of this study is to test the suitability and added value of XCS for environmental geochemical characterisation on cores that contain a heterogeneous series of sediments. A further challenge arises from the core being stored at ambient room conditions for a prolonged time and scanned post-sampling for conventional geochemical analyses. This study highlights the advantages as well as the limitations of the XCS-MLC method to rapidly analyse sediments that are heterogeneous in sedimentary facies, lithology and mineralogy. We show results for a wide range of elements with focus on reactive iron, calcium carbonate and sulphur, as these parameters are often used to track environmental and diagenetic changes in sediments and soils with depth.

2. Material and methods

2.1. Samples, sample preparation and XRF core scanning

Four Holocene to Pleistocene sediment cores from the Western Netherlands (cored in 2008–2009) were retrieved for XCS from the TNO Geological Survey Netherlands core repository, where they were kept at ambient room conditions. The core locations are shown on the map in Fig. 1. The lithological and stratigraphic descriptions are digitally available from the DINOloket website (www.dinoloket.nl) of TNO Geological Survey Netherlands. The sediments studied comprise fluvial, fine to coarse sand deposits (Pleistocene Waalre, Urk, and Kreftenheye Formations) and finer sand to silt deposits (Holocene Echteld Formation) of the Rhine river system (De Gans, 2007). The riverine deposits interfinger with marine calcareous sands and silty clays of the Holocene Naaldwijk and the Pleistocene Eem Formations, as well as the Holocene peat deposits of the Nieuwkoop Formation. During the Saalian, the northern half of the Netherlands was covered with ice leading to the development of the glacial Drente Formation. The Pleistocene/Holocene Boxtel Formation contains predominantly aeolian and lacustrine sands and loess; it typically lies on top of the Pleistocene fluvial and marine sediments and under the Holocene, fluvial, marine and peat deposits. The main detrital components of the Holocene and Pleistocene sediments are quartz, clay minerals (predominantly illite and smectite), mica (mostly muscovite), feldspar (mostly orthoclase), calcite shells and lithic fragments (Breeuwsma, 1990). The dominant secondary minerals are calcite, siderite, pyrite and Fe-oxyhydroxides and presumably Al-oxyhydroxides (Griffioen et al., 2016).

Core selection was based on acquiring a broad range of lithological and geochemical compositions. Core B25E1030 (16 m) has a high sample resolution and the sediment is rich in carbonate, pyrite and organic matter. Core B25G2090 (34 m) is also rich in pyrite and peat but has the lowest carbonate content. Core B42E0748 (30 m) was selected as a sand-rich example with low to medium carbonate content. The sediments have little pyrite with only a few samples containing significant iron. Core B43B0660 (40 m) has a high clay content, several organic carbon-rich layers, partially related to peat deposits, and a carbonate-rich layer.

The geochemical analyses on discrete samples were performed between 2009 and 2011 at the TNO-Deltares geochemical laboratories (Utrecht; The Netherlands), i.e. prior to core scanning. The element concentrations of the samples are used as a reference dataset for the MLC calibration. For the geochemical analyses, ~50 ml of sediment was sampled from ~5 cm length from different lithological layers along the core. In total, 50 samples were collected from core B251030, 39 from core B25G2090, 27 from core B42E0748 and 32 from core B43B0660 (Table S1). Most commonly, one sample per meter was collected in order to obtain a sufficient number of samples per combination of geological formation, sedimentary facies and lithological class for the entire series of 47 drillings in Western Netherlands (cf. Van Gaans et al., 2011; Griffioen et al., 2012). The samples were always collected from stretches that visually looked homogeneous in lithology, i.e., the lithological layer sampled had to be thicker than the sampled interval. For all but peat samples major, minor, and trace elements were measured via wavelength-dispersive X-Ray Fluorescence (XRF). The XRF measurements were conducted on either pressed powder pellets or fused beads

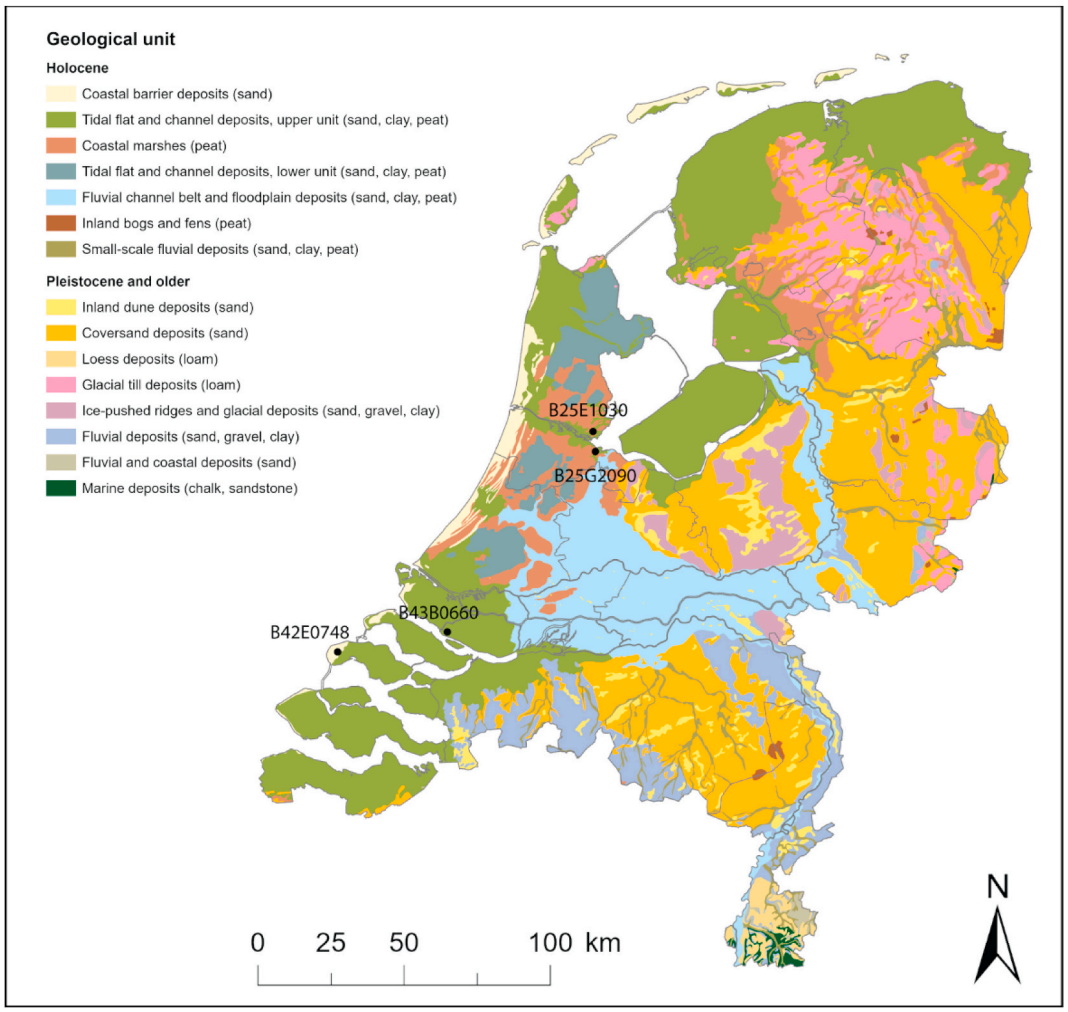

Fig. 1. Surficial geology of the Netherlands with core locations (black dots).

(Supplementary Table S1) on an ARL9400. For the peat samples the element composition was measured via inductively coupled plasma spectrometry (ICP) following total sample destruction (hot $HF/HNO_3/HClO_4$ digestion). Major and minor element analyses were performed on an ICP-Optical Emission Spectrometer (Spectro Ciros ICP-OES) and trace elements on an ICP-Mass Spectrometer (Agilent 7500a ICP-MS). Repetitive measurement of standard material ISE921 showed that the accuracy was between 3 and 10% (2 sd) for XRF measurements and 5–15% for ICP measurements (van de Veer, 2006). The analytical precision based on duplicate sample measurements was better than 10% (2 sd) for XRF measurements and better than 5% (2 sd) for all ICP measurements, except for Zr (10%, 2 sd). For the majority of the samples, S was measured via combustion and infrared detection on a LECO SC-632 element analyser and for the remaining samples via XRF on pressed powder pellets. The analytical standard precision for S was better than 10% (2 sd). Accuracy, on the other hand, was low for both XRF (37%, 2 sd) and LECO (63%, 2 sd) for S (van de Veer, 2006). Organic matter was measured thermogravimetrically (LECO TGA701) at temperatures from 105 to 550 °C (relative standard precision better than 5%, 2 sd) and corrected for clay (van Gaans et al., 2011) that was determined by grain size analyses (Malvern Mastersizer) with a standard precision better than 10% (2 sd).

A verification dataset of 38 samples was taken from the four cores in 2019 (post core-scanning) and analysed at the German Centre for Geosciences (GFZ). The sampling strategy was to take about ten equidistant samples per well. For the cation analysis the samples were digested via 4 acid method (hot aqua regia/$HF/HClO_4$) in Savillex® PFA beakers (Savillex Corp., Eden Prairie, USA) using ultrapure reagents. The elements Al, K, Ca, Ti, Mn, and Fe were measured on ICP-OES (5110, Agilent Technologies, Santa Clara, USA). The relative uncertainty on Al, Ca, Fe, Mn and Ti was better than 5% and on K 10%. The trace elements As, Cr, Ni, Cu, Zn, Rb, Sr, Zr, Ba, and Pb were measured using high resolution ICP-MS (ELEMENT 2XR, Thermo Scientific, Waltham, USA) with a relative uncertainty better than 2%, except for As, which had an uncertainty of 3%. Instrumental drift was corrected for using In as an internal standard. Total sulphur was measured via an Eltra 2000 CS Analyser. The relative uncertainty was better than 10% for S. Organic carbon was analysed on a Flash HT 2000 Organic Elemental Analyser, following a 6 M HCl digestion of carbonate at 70 °C. The error was less than 10% (RSD) for TOC, based on the reproducibility of reference materials and sample duplicates. Total organic carbon (TOC) was used to calculate the organic matter content in the verification dataset by multiplying TOC with a factor of 1.9 (Klein and Griffioen, 2010).

X-Ray Fluorescence core scanning was performed with an Avaatech core scanner at the Royal Netherlands Institute for Sea Research (NIOZ). Before XCS analysis, the sediment surfaces of the cores were carefully flattened, and covered with a thin (4 μm) Ultralene foil. The XRF scanning was performed with a 100 W rhodium (Rh) X-ray tube and with a Canberra silicon drift detector. To cover the full range of elements from Al to Ba we used the following three tube energy settings: 10 kV for Al to Fe, 30 kV for Co to Rb, and 50 kV for Sr to Ba with, respectively, no filter, Pd-thin filter, and Cu filter, which were measured for 20 s, 20 s, and 40 s, respectively. The X-ray source current was selected to maintain a detector throughput with preferably ~20–30% dead time (Table 1).

Table 1
The XRF-core-scan settings used on the core material.

Resolution i.e., step size (mm)	Cross-core slit opening (mm)	Down-core slit opening (mm)	X-ray Source voltage (kV)	Energy (mA)	Live time (s)	Filter
10	12	10	10	0.75	20	–
10	12	10	30	0.50	20	Pd-thin
10	12	10	50	1.5	40	Cu

Nonetheless, the dead time was sometimes lower in sediment layers with abundant organic material (peat). The core material was measured with 1-cm resolution, excluding sections that contained none or too little material. The irradiated area of the X-ray beam was set at 1 cm ("down core") by 1.2 cm ("cross core") using the slit settings of the scanner. The spectral data were processed using WinAxil spectrum analysis software, which translates the spectral data into element intensities (in counts).

For consistency control we measured the South African Reference Material SARM-4 standard tablet (The Council for Mineral Technology, MINTEK) before and after every run (n = 113) at 10 kV. Moreover, we measured a SARM-4 and PACS-2 (National Research Council of Canada) standards, at the three used settings on a weekly basis (n = 7). The reproducibility (precision; calculated as Relative Standard Deviations) of the elements was monitored. The standards showed a precision for the elements (SARM-4; PACS-2): Al (4%; 3%), Si (4%; 4%), S (25%; 3%), K (15%; 2%), Ca (1%; 1%), Ti (5%; 1%), Cr (7%; 11%), Mn (3%; 5%), Fe (1%; 1%), Ni (6%; 25%), Cu (21%; 1%), Zn (5%; 1%), As (9%; 8%), Br (4%; 1%), Rb (17%; 5%), Sr (2%; 2%), Zr (7%; 1%), Ba (6%; 2%), Pb (9%; 2%). These repeated analyses throughout the measurement series showed that the reproducibility was high (<10%) for most elements, as long as they were abundantly present (i.e., present in concentrations above the detection limit) in the standard samples. Hence, the setup and performance of the XRF core scanner remained stable for the entire duration of the experiment.

2.2. Calibration of the XCS data

The XCS data are initially presented as intensities (counts), which is the output from the WinAxil software. However, bias in XCS intensities occurs due to variability in physical sediment properties, measurement geometry (i.e., the XRF sampling space including the sample itself, water content and film, thin foil, and measurement unit with X-Ray source and detector), and non-linear matrix effects (i.e., all elements present in the sampling matrix that may enhance/absorb fluorescence of an element of interest). These effects can largely be corrected by the MLC model (Weltje et al., 2015), which is especially necessary for this core material as it consists of very contrasting sediment matrices and was also strongly dehydrated during prolonged storage (affecting the smoothness of the sample surface and resulting in abundant crack formations). We note that this calibration method has significant advantages over less sophisticated calibration methods (e.g., simple linear calibration or the univariate log-ratio calibration of Weltje and Tjallingii (2008)), as it is unique in its capability to correct matrix effects and predict "absolute" concentrations for elements by incorporation of the element fraction that cannot be measured directly (i.e., the undefined or "undef" fraction). Using this undefined fraction, ensures that the total sum of all elements combined is always 100% with the MLC approach.

The MLC of the XCS data (n = 9847) was performed with the AvaaXelerate software (Bloemsma, 2015). The data for the four cores were calibrated together, because the sedimentary matrices and their heterogeneity were similar among the cores from the different wells. For calibration, we used the reference dataset that was analysed between 2009 and 2011, prior to the core scanning (Supplementary Table S1). Due to the removal of core material for discrete sampling, the cores had missing intervals that could not be scanned. In part, only the central part of the core was collected for the discrete sampling, leaving enough sediment for the scanning next to these samples. As the XRF core scanning was done after the discrete sampling, we matched the calibration data depths to the depths in the core scan as close as possible, with a maximum of ±3 cm to the mid-depth of the sampled interval (Supplementary Table S1). Samples outside of the ±3 cm interval were omitted, resulting in a reference dataset of 129 samples. The conversion of intensities into contents was done for Al, Si, S, K, Ca, Ti, Cr, Mn, Fe, Ni, Cu, Zn, Rb, Sr, Zr, Ba, and Pb, combining data that were measured during three separate runs with different voltage settings during XCS. The samples have a different number of conventionally measured elements due to different geochemical analyses being ran on different samples for the reference dataset (see table S1). This resulted in a different number of calibrated values for each element.

We preferred to exclude As and Br in the simultaneous calibration of all the other elements, because calibration for both these elements has not yet been established and including them in the 100% sum of totals may otherwise affect all other elements. The latter is especially true for the Br to organic carbon calibration, as the peats have high organic carbon contents with a large effect on the closed-sum constraints in this calibration approach. As these two elements may hold important environmental information, we performed two separate calibration runs with the remaining 17 elements (see above) including either As and Br (18 in total for each run). Additionally, we performed a background correction for As, because As showed a large amount of negative values, which otherwise could not be calibrated with the MLC approach. We performed this correction using the output intensities for As from WinAxil and adding 6000 counts to make all intensities >500 counts.

2.3. Chemometric calculations

Total Fe may be distinguished in reactive Fe (such as oxides, siderite, sulphides) and non-reactive Fe. Non-reactive iron is considered as silicate-bound Fe, mostly occurring in clay and heavy minerals and can be calculated with the aid of Al contents. The underlying assumption is that silicate-bound Fe_2O_3 amounts to ~22.5% of total Al_2O_3 content (Huisman and Kiden, 1998; Dellwig et al., 2001, 2002) that was calculated as follows:

$$Fe_2O_3(\text{non-reactive}) = \alpha \text{ x } Al_2O_3 + \beta \quad \text{Eq. 1}$$

Where α and β are empirically determined coefficients for each formation (Heerdink and Griffioen, 2008; Griffioen et al., 2012). The relation between non-reactive Fe and Al is different for Al_2O_3 contents >5% compared with contents <5%. This is due to the dominance of feldspars and heavy minerals in the silt and sand fraction and that of clay minerals in the clay fraction (Huisman and Kiden, 1998; Griffioen et al., 2012). Note that non-reactive Fe can also be present in heavy minerals, which do not contain Al and weather slowly. Furthermore, the presence of glauconite may cause variations in the Fe content, although its presence is usually limited to particular formations (Odin and Matter, 1981; Amorosi et al., 2007).

Calcium carbonate was calculated from the Ca content using an empirical formula to subtract silicate-bound Ca (in particular as Ca feldspar) with the aid of the Al content (Bakker et al., 2007; Griffioen et al., 2012):

$$\text{Ca-carbonate} = 1.78 \times [CaO - (0.0448 \times Al_2O_3 - 0.1147)] \quad \text{Eq. 2}$$

Calcium can also be present as sorbed Ca^{2+} and as Ca bound in dolomite, Mg-bearing calcite and ankerite, whose presence would either increase or decrease the calculated Ca carbonate content. The calculated Ca carbonate content should thus be seen as an estimate and not as face value. Total reactive Fe and $CaCO_3$ were calculated for both the conventionally measured and MLC-XCS data, using equations (1) and (2).

3. Results

The lithology as well as the mineralogy and element contents vary considerably in the four cores as indicated by the results of both the discrete samples from the reference dataset and the continuous core scanning (e.g., Fig. 2, S1). Elevated element contents of FeTR, TS, Ni, As, Zn and Cr are found mainly in the peat and clay-rich sediment. Calcium and $CaCO_3$ is generally higher in the marine Naaldwijk and Eem deposits than in other deposits, which may be connected to the inclusion of shells or shell fragments during deposition (Griffioen et al., 2016). The fluvial Waalre Formation also contains a carbonate-rich level in core B43B0660 (Fig. 2). Aluminium and K correlate well in the four sections. Their contents are generally higher in peat, clay and loam than in sand deposits, but the content does not always correlate with the lithology as they are present together in clay-sized illite and often silt-sized K-feldspar (Boggs, 2009), which are both common sedimentary minerals.

A comparison of the analytical data reveals that the MLC calibrated element contents are more consistent with the data from the reference

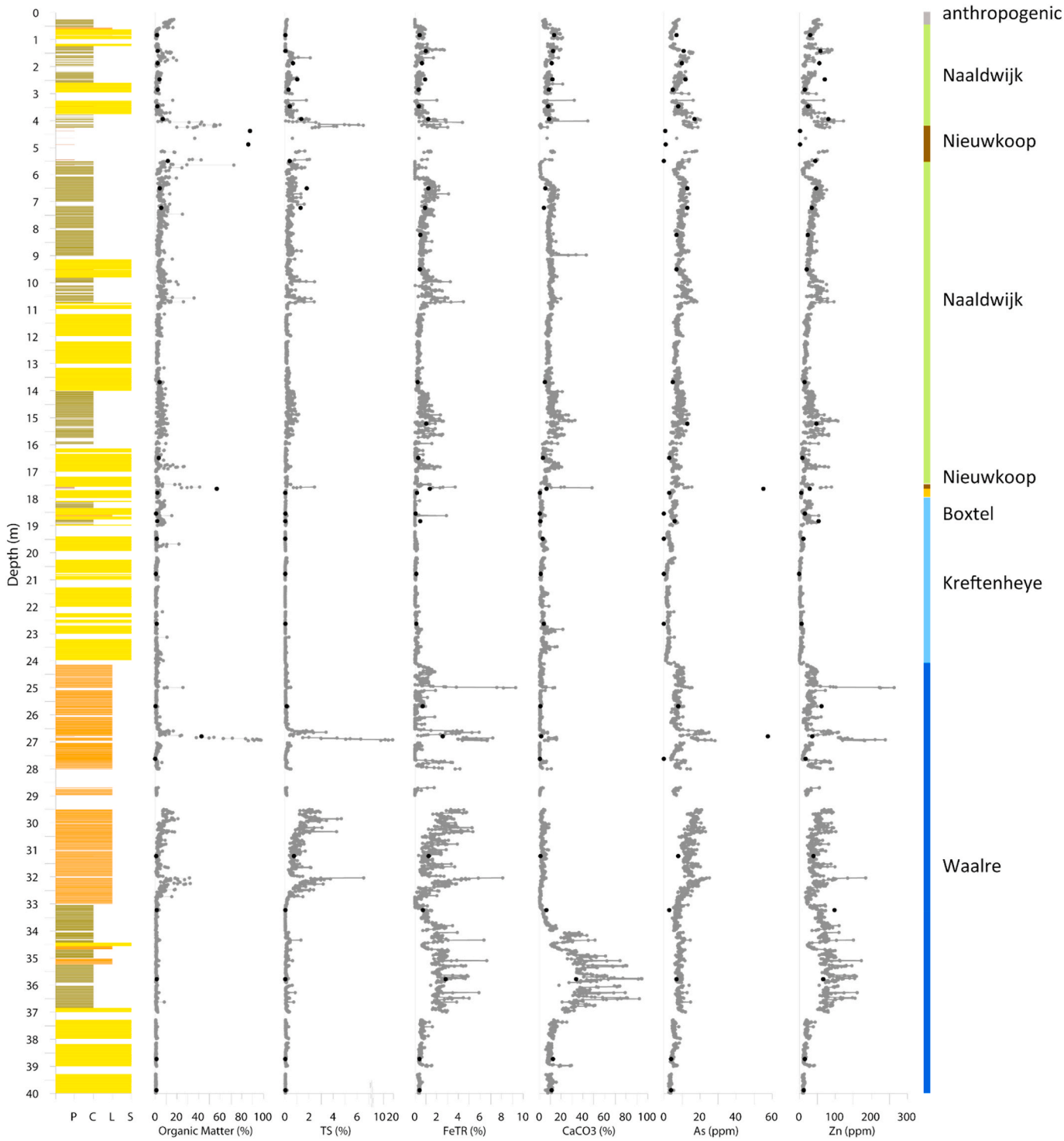

Fig. 2. Geochemical depth profiles for core B43B0660 with classification of lithology (P = peat, C = clay, L = loam, S = sand) and geological formation in the right column. The grey lines represent MLC-XCS data and the black dots conventionally measured data.

Table 2
Pearson correlation factors of reference data compared to raw intensities (R^2 raw-reference), XCS-MLC values for the calibrated samples and reference data (R^2 MLC-reference), MLC calibrated values and the verification dataset (R^2 MLC-verification), and MLC calibrated values compared to the combined reference and verification datasets (R^2 MLC-conventional).

	Al	As	Ba	Ca	Cr	Cu	Fe	K	Mn	Ni	Pb	Rb	S	Si	Sr	Ti	Zn	Zr	Br/org.matter
R^2 raw-reference	0.17	0.39	0.28	0.05	0.00	0.01	0.01	0.14	0.55	0.00	0.04	0.04	0.37	0.11	0.37	0.11	0.61	0.52	0.01
R^2 MLC-reference	0.72	0.27	0.42	0.58	0.77	0.25	0.70	0.59	0.62	0.45	0.62	0.65	0.72	0.68	0.51	0.74	0.53	0.55	0.87
R^2 MLC-verification	0.77	0.47	0.29	0.49	0.71	0.13	0.80	0.56	0.48	0.74	0.36	0.55	0.74	n.a.	0.56	0.84	0.54	0.62	0.73
R^2 MLC-conventional	0.73	0.28	0.39	0.55	0.75	0.15	0.72	0.58	0.58	0.48	0.49	0.62	0.70	0.68	0.51	0.76	0.53	0.55	0.86

dataset, compared to the raw intensity data (Fig. 3, S2; Table 2). Noteworthy is the much larger intensity variability in the raw XCS data for most elements compared to the much more constant concentrations (i.e. less variability) seen in the MLC calibrated values (e.g., see the much larger intensity range in Ca and S at 5–9 m depth in Fig. 3, or similarly the range in Cr at 25–34 m depth in Fig. 3). This is likely related to measurement geometry differences, such as the unevenness of the measurement surface due to dehydration of the core causing variable

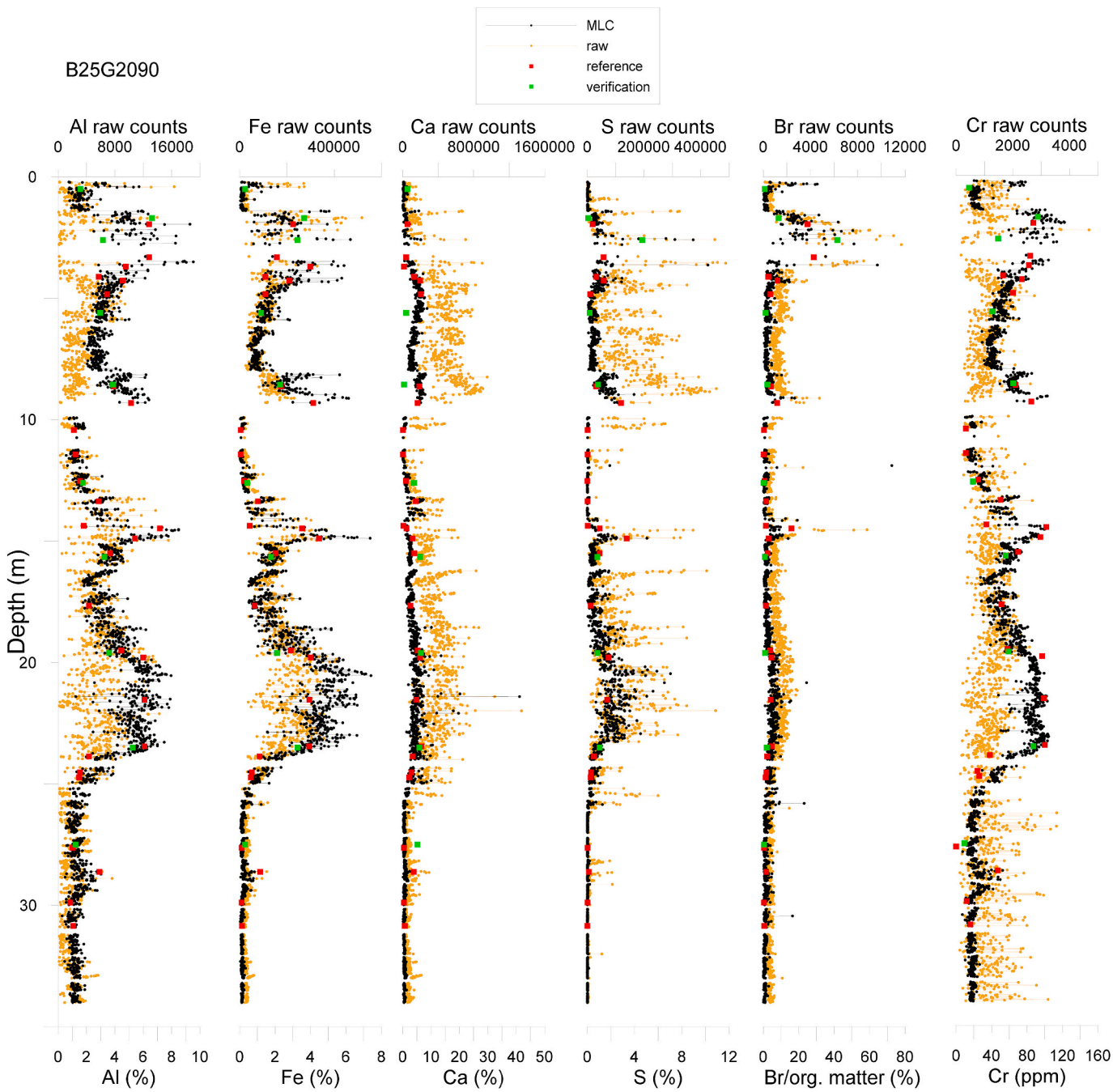

Fig. 3. Comparison of raw intensity values, MLC-calculated values, reference values from the reference dataset (red squares) and the verification dataset (green squares) for core B25G2090 for some environmentally relevant elements. (For interpretation of the references to colour in this figure legend, the reader is referred to the Web version of this article.)

amounts of air to be part of the XCS measurement. The latter can cause large variability in raw intensities, yet, our data shows that such variability is sufficiently corrected for by the MLC calibration method. The MLC-calibrated data therefore concurs much better with the reference and verification data sets (e.g. Fig. 3). A good positive correlation ($R^2 > 0.6$) was achieved between the reference values and the MLC values for Al, S, Si, Fe, Mn, Ti, Rb, Pb, Cr and also for Br as proxy for organic matter (Figs. S3; Table 2). The correlation factors for Sr, Zr, K, Ni, Ba, Zn and Ca are lower but within reasonable range (between 0.4 and 0.6) and Cu and As have poorer correlation factors of <0.30 between the two datasets. Due to error propagation, the correlation between the calculated Fe-TR and $CaCO_3$ for reference values and MLC values is reduced compared to the correlation for the elements themselves (Fig. 4).

The element contents deviate randomly around the identity line between the MLC and reference values (Fig. S3). Outliers can be recognised for several elements. For example, by removing three exceptionally high (>40 ppm) arsenic reference values the correlation improves to $R^2 = 0.61$ (Figure S3). These outliers do not seem to be related to a specific lithology, analytical technique for the reference values, or core. Overall, the consistency between the reference and the MLC data proved to be independent of the grain-size.

The MLC calibrated data was subsequently compared to the 'verification dataset' that was measured in 2019 at GFZ (Supplementary Table S2) to determine how well the MLC-XCS data compares to a dataset that was not used for its calibration. Strong correlations ($R^2 > 0.6$) between the MLC-XLS and test dataset were achieved for Al, Cr, Fe, Ni, S, Ti, Zr and Br (vs. organic matter). Moderate correlation factors of between 0.4 and 0.6 were calculated for As, Ca, K, Mn, Rb, Sr and Zn (Table 2) and a poor or no correlation ($R^2 < 0.4$) was evident for Ba, Cu and Pb. Although the correlation for Zr was good, the line of linear regression deviated from the identity line (Figure S4). Zircon may not be fully digested in a 4-acid solution (e.g., Yamasaki et al., 2016), which would explain the consistently lower values for ICP-MS compared to the MLC-XCS technique. The Zr values of the verification dataset will thus not be used in further discussion. Compared to the calibrated dataset, the correspondence between the verification dataset and MLC-XCS improved for Al, As, Fe, Ni, Ti and Zr, slightly worsened for Ba, Ca, Mn, Pb, Rb and Br/organic matter, and was similar for Cr, K, Sr and Zn.

4. Discussion

4.1. Calibrated XCS data versus conventional data

The XCS-MLC calibration method is a statistical approach to transform raw data to actual elemental concentrations (Weltje et al., 2015). For our purposes, in which the data is to be applied in an environmental geochemical context, such a transformation is a prerequisite. An important benefit from XCS is that the continuous scanning enlarged the down-core spatial resolution and hence the dataset increased from 148 to 9897 data points. The correspondence between the conventionally analysed data and the MLC-XCS data was generally good. Possible errors to the calibration method may have been introduced by the different preparation or analysis of the reference samples (XRF-bead, XRF-pellet and total digestion with ICP analysis) and high standard errors for some elements (e.g., S). Another reason for a less good correlation between the reference and the MLC-XCS datasets is a spatial difference in sampling, with discrete samples having a size of about 5 cm and the scanning range for one XCS measurement being 1 cm. Based on the rapid high frequency intensity changes observed down core (e.g., Fig. 3, core B25G2090 1.5–4 m and 9–10 m), this factor possibly introduces the largest mismatch between the XCS and the conventionally measured data.

Importantly, the geochemical variability observed in the XCS-MLC data is a much better representation of the real geochemical variability than the intensities alone, as indicated by the conventional geochemical data (e.g., see 0–4 m depth in Al in Fig. 3). These data show that the MLC approach of Weltje et al. (2015) significantly improves XCS results due to corrections implemented within this approach (e.g., correcting enhancement/adsorption effects on intensities and dilution effects caused by the peats). The generally high correspondence between MLC-XCS data and the verification dataset confirms the improvement of the XRF-scanning data (Fig. 3; Table 2). The lower correlation

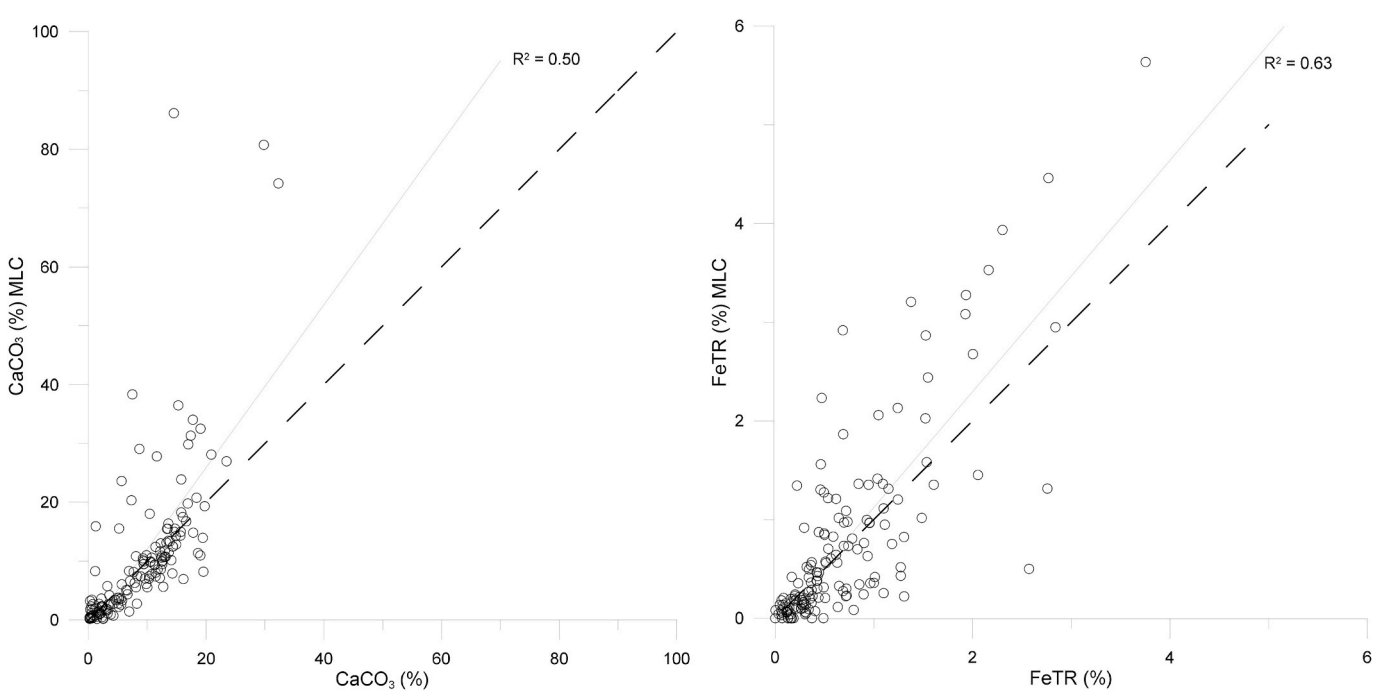

Fig. 4. Correlations for calculated $CaCO_3$ and FeTR contents between conventional techniques (combined reference and verification datasets) and the MLC-XCS technique. The dashed line is the identity line.

coefficients for some elements compared to the calibrated dataset can be related to a lower number of values that were available for the correlation (38 versus 129 samples). Considering that correlation coefficients were similar between the reference-XCS-MLC and the verification-XCS-MLC datasets and even significantly improved for As, Fe, Ni, Ti and Zr for the verification-XCS-MLC correlation (Figure S3 and S4), it is reasonable to conclude that the MLC was applied appropriately. The overall correspondence between the conventionally measured values and the XCS-MLC values is remarkably robust in the cross-plots (Figure S3 and S4) and down core (Figure S2). When comparing both the reference and the verification datasets with the MLC values, an acceptable correspondence ($R^2 > 0.5$) is achieved for Al, S, Si, Fe, Mn, Ti, Pb, Rb, Cr, Sr, Zr, K, Ni, Zn, Ca and Br/organic matter. Arsenic, Ba and Cu have poorer correlation factors and therefore should be used with care in such heterogeneous cores. This may be surprising, as other studies have shown good correlations for at least Cu (e.g. Weltje et al., 2015) and Ba (e.g., Grant et al., 2017). Yet, in our case the concentration range of these two elements is relatively low (i.e., generally between 5 and 15 ppm for Cu and 150–250 ppm for Ba; see Figure S3) compared to these other studies (200–1000 ppm for Cu in Weltje et al. (2015) and 0–3000 ppm for Ba in Grant et al. (2017)). As such, at least part of the poor correlation for Ba and Cu can be assigned to the relatively low range in our dataset. At present, limited data is available for As. It is possible that low concentrations and the low concentration range are resulting in the poor correlation for As but it is noteworthy to indicate that R^2 increases to 0.61 when three outlying values are removed (see Figure S3). This indicates that valuable environmental information can still be retrieved from As intensities, even though the initial intensities were negative (see section 2.2).

Bromine is regarded as a good indicator for marine organic matter in sediments (Ziegler et al., 2008), but has not been assessed for terrestrial organic matter (in particular peat). Hence, we explore here the use of Br to estimate the organic matter content in this core material. The observed correlation between organic matter and calibrated Br contents was remarkably high ($R^2 = 0.87$ for reference dataset and $R^2 = 0.73$ for verification dataset), which indicates that Br has high potential to also be used as a proxy for organic matter in terrestrial and peri-marine sediments. However, as Br is generally notably higher in marine organic matter compared to terrestrial organic matter (Ziegler et al., 2008), it remains to be investigated if such a calibration can be applied to other datasets with sediments of both terrestrial and marine origins.

The MLC-XCS method resulted in some particularly high element contents for Ca, Fe and S, compared to the conventionally measured values (Fig. S2). Ca contents of > ~40% are inconceivable as they are equivalent to more than 100% calcium carbonate in the sediment. Although shell debris is mentioned in the core descriptions for the high Ca intervals, the shells cannot be fully responsible for the high values. Total sulphur (TS) contents of >8% are unusual for Holocene or Pleistocene onshore sediments of The Netherlands (Huisman and Kiden, 1998; Griffioen et al., 2016). Nevertheless, TS contents of up to 13% have been measured in comparable Holocene peat deposits in Northwestern Germany and Western Denmark (Postma, 1982; Dellwig et al., 1999). Total Fe contents in Holocene and Pleistocene sediments generally do not exceed ~5%. However, anomalously high Fe contents of up to 25% were occasionally observed as a product of siderite formation (Griffioen et al., 2016). Grant et al. (2017) also noted that anomalously high element contents (e.g., Ba) were produced by the MLC-XCS method. The MLC approach can overestimate the high-end values, especially if conventional analyses are not available for calibration from the corresponding intervals. This is due to high XCS values falling outside of the calibration range and thus needing to be extrapolated.

The range in the conventionally measured values is similar to that in the MLC-XCS values for the majority of the elements, for example for Al and Ni (Fig. 5). This indicates that the conventionally measured samples are generally representative of the entire dataset and serve as a validation of the regional-scale methodology proposed by Van Gaans et al. (2011) and Griffioen et al. (2012). In some cases, the frequency distributions are systematically different. Although, for example, S distributions are similar between the two datasets, the values are much higher in the MLC-XCS dataset compared to the reference dataset (Fig. 5). As mentioned previously, this is due to a possible MLC overestimation of high-end values due to lacking high-end conventionally measured values. For Pb, Cu and Br the distribution of the values is different between the MLC-XCS and the reference values (Fig. 5). For Pb and Br, the conventionally measured values likely did not cover the actual spread of concentrations in the cores that was achieved by the high-resolution XCS data. This may not be the case for Cu, as the XCS-MLC data did not correlate well with conventionally measured Cu values ($R^2 = 0.15$). Overall, we assume that the vast majority of the MLC-XCS data reflects the true distribution of the element contents due to the sheer number of MLC-XCS values compared to the conventionally measured data.

Although the correlation between the MLC and the conventionally measured data is reasonably good, other studies (Weltje et al., 2015; Grant et al., 2017; Falster et al., 2018; Gregory et al., 2019; Hennekam et al., 2019) often achieve correlations with less scatter around the identity line (i.e., Fig. S3). The reasons for the better correlation in those studies compared to this study is related to the large mineralogical and grain-size homogeneity of the sediments compared to the series of sediments in this study (from sand to peat), as, XCS is best performed on relatively small (clay to silt) grain size (Richter et al., 2006). Most other studies focus on more homogenous material and it is possible that the MLC approach does not sufficiently correct for all these large matrix changes, although it clearly provides a significant improvement over using raw intensities. Moreover, XCS is generally performed on fresh cores with smooth surfaces. The cores at hand were stored in boxes at ambient room conditions and were not subjected to temperature and humidity regulation. This led to dehydration cracks in parts of the cores, which would have suppressed XCS signals as sampling surfaces were not always optimally flat and cracks could not always be avoided (i.e. thus sometimes measuring partially air and sediment).

Another shortcoming of analysing older cores is that they are often extensively sampled resulting in less direct overlap for calibration. Discrete sampling after, instead of before, XRF scanning is thus preferred, as it allows incorporating the full concentration range for every element within the calibration. Post-scan sampling would also offer the opportunity to use the superior automated sample selection option in AvaaXelerate, which optimizes the effectiveness of the calibration samples while minimizing the sample amount needed (Bloemsma, 2015; Weltje et al., 2015). Nevertheless, the results of this study indicate that meaningful concentration data for environmental purposes can be obtained from sediment material that was not optimally stored and sampled.

4.2. Geochemical characterisation of vertical heterogeneity

Many sediments are heterogeneous by nature and a relevant question is whether high-resolution scanning adds information compared to low-resolution sampling. Below, we compare the environmental insights

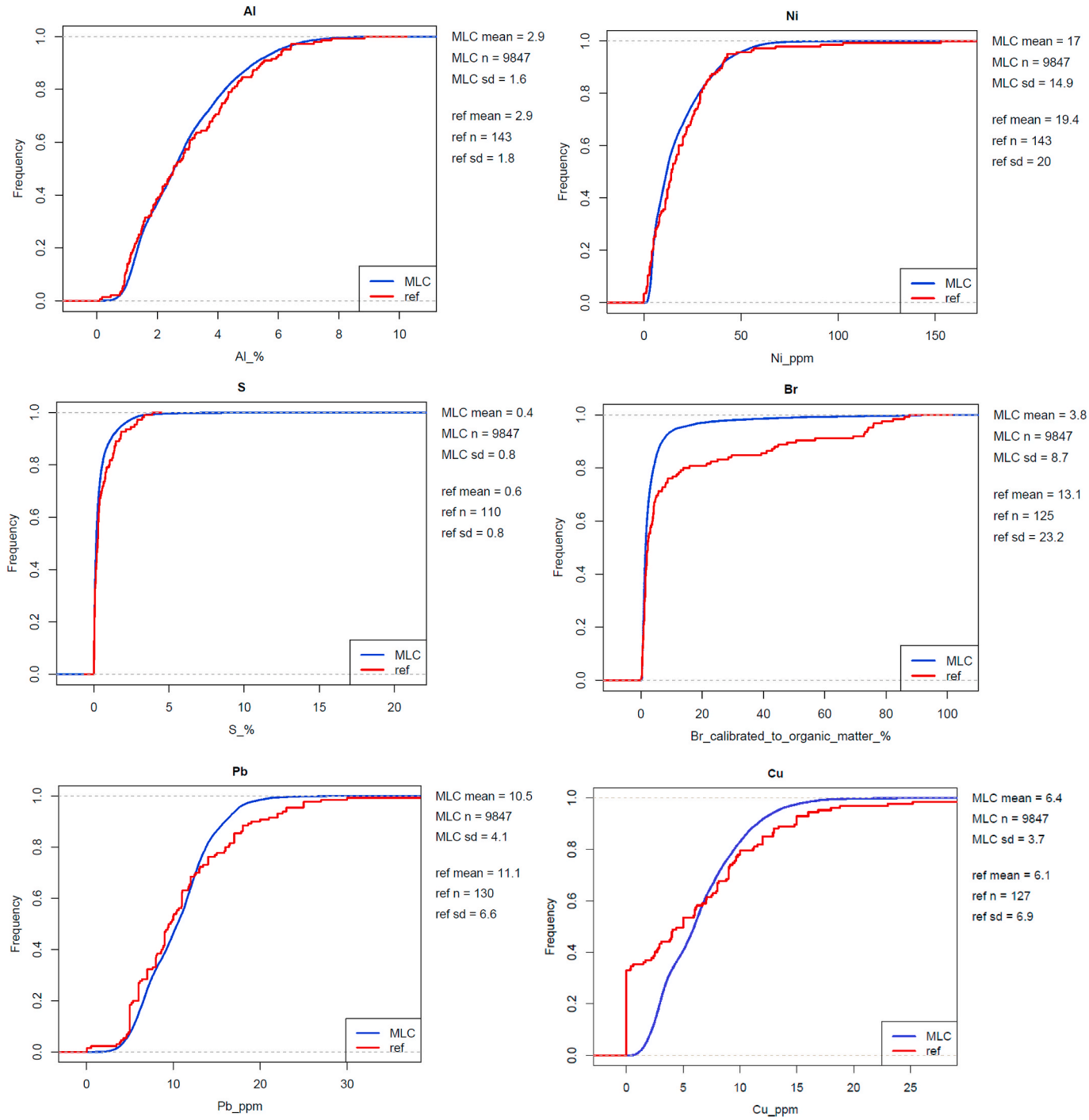

Fig. 5. Frequency plots of the elemental contents as determined by the conventional techniques and the MLC-XCS technique for Al, Ni, S, Br/organic matter, Pb and Cu.

gained from the conventionally measured data from the reference dataset to the MLC-XCS acquired data for the four studied cores.

In core B25G2090 the conventionally measured values correspond well with the MLC-XCS values (Fig. 6; S1). The general trends of the element and mineral compositions shown by the MLC-XCS data are also recorded by the reference data. A few high MLC-XCS values were not represented by reference measurements (high TS, FeTR and organic matter at 3.6 m; several $CaCO_3$ peaks between 21.5 and 22.5 m; high Zn values at 3.9, 8.8 and 19.3 m). The strikingly high values could be outliers caused by a lack of calibration for the entire data range (see

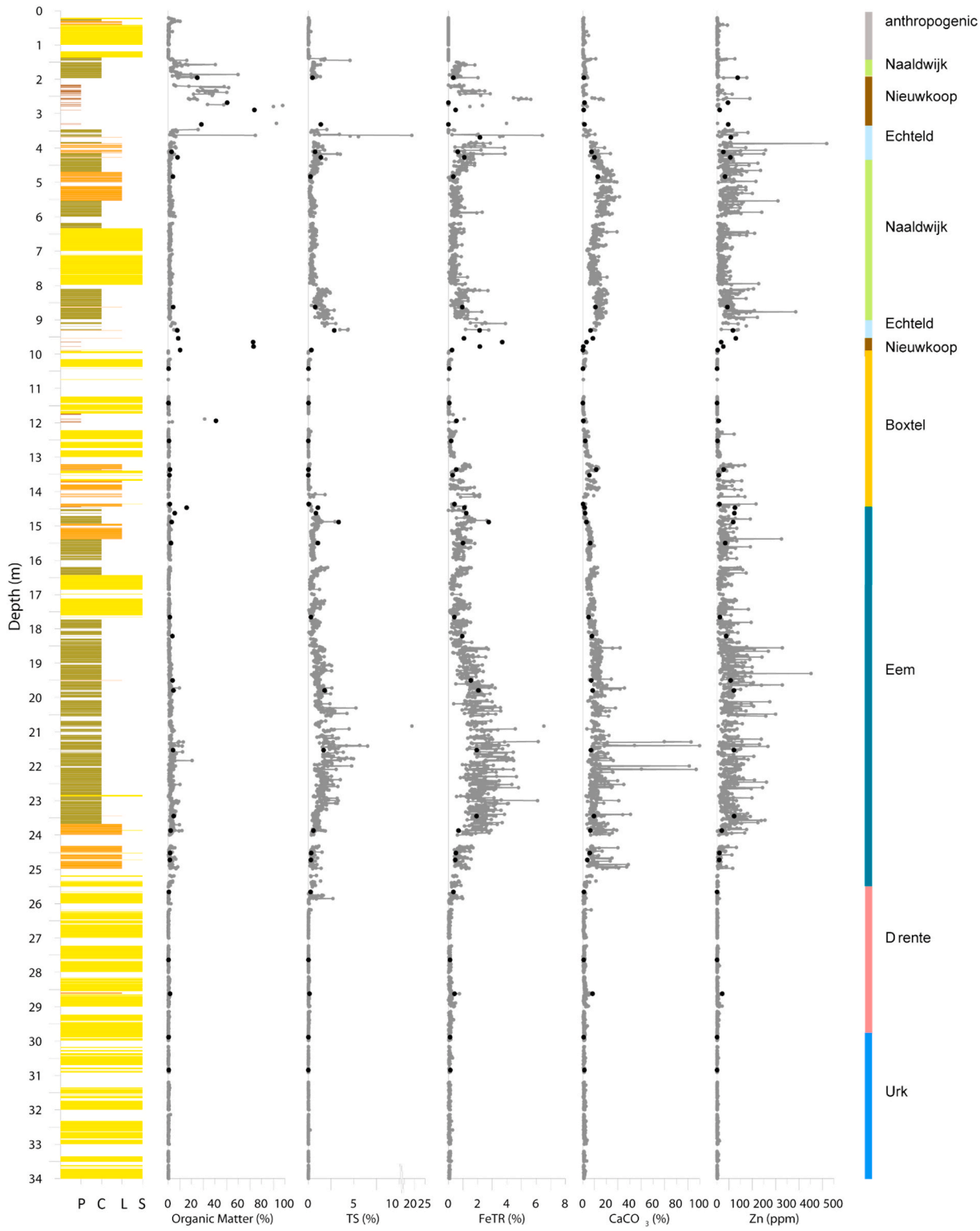

Fig. 6. Geochemical depth profiles of core B25G2090, with classification of lithology (P = peat, C = clay, L = loam, S = sand) and geological formation. The grey dots and lines represent MLC-XCS data and the black circles conventionally measured reference dataset.

discussion in previous section). Alternatively, they may represent small accumulations of shell material for Ca and pyrite minerals for S and Fe, as well as Fe-oxyhydroxides. Even if the peaks represent true contents, singularities are not of primary interest for environmental interpretations.

Core B25E1030 contains three distinct intervals of reactive mineral and environmentally viable trace metal enrichments. In the lower Naaldwijk to Nieuwkoop Formation interval (~12 m depth) peat and humic clay sediments are enriched in FeTR, TS, Mn, As, Zn and Ni (Fig. 7). Calcium carbonate is also high (Fig. S2), which is partly related to abundance of calcite shells. Calcite was calculated on the basis of the calcium content; however another carbonate source of Ca can be ankerite and dolomite. Both Mn and Fe contents are elevated in this interval, therefore both minerals can potentially contribute to the

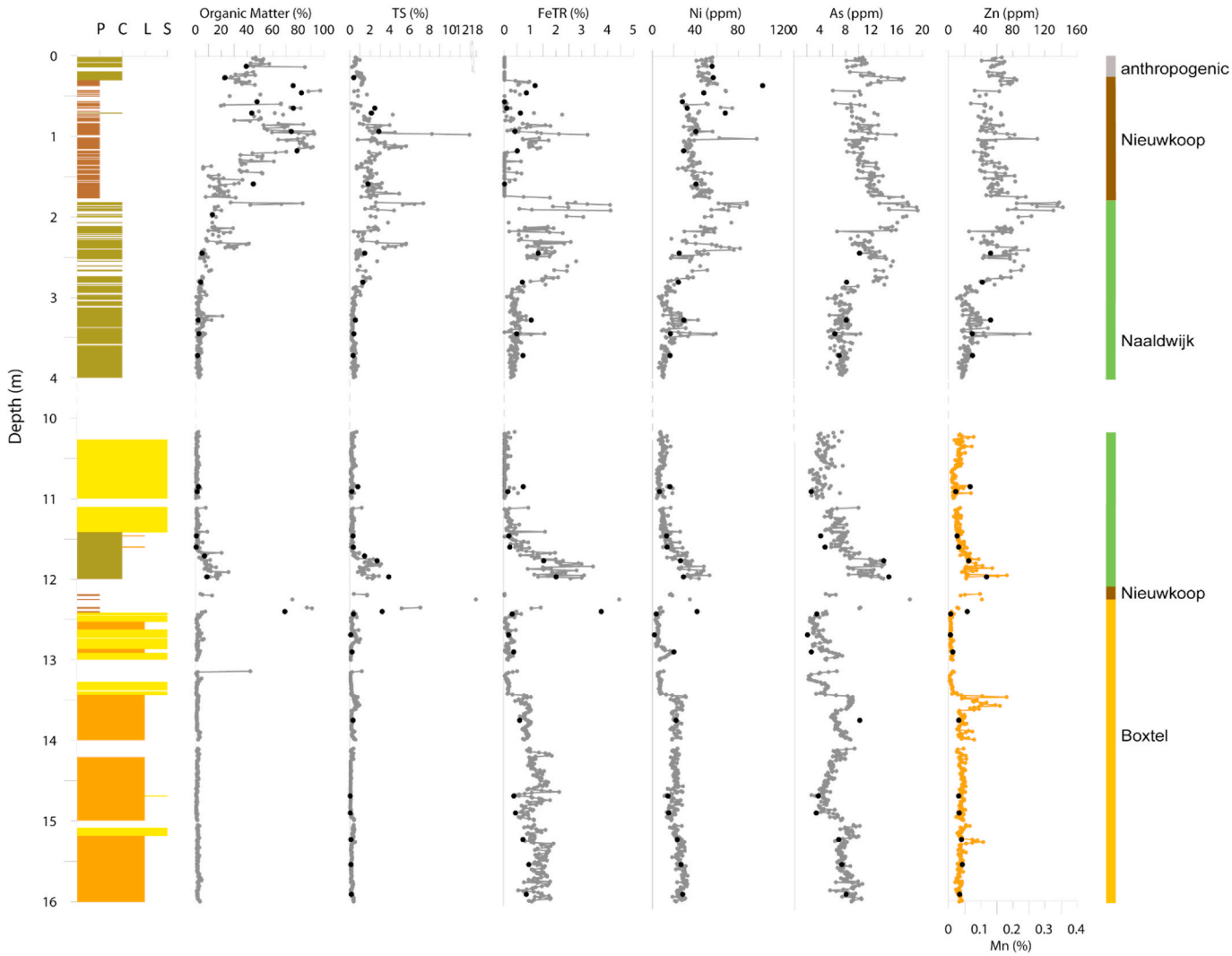

Fig. 7. Geochemical depth profiles for part of core B25E1030 with classification of lithology (P = peat, C = clay, L = loam, S = sand) and geological formation. The lines represent MLC-XCS data and the black circles conventionally measured reference dataset. Manganese is shown in beige and Zn in grey. The dashed lines represent 6.3 m of the core that are not shown in this figure.

calcium carbonate fraction. A fair correlation ($R^2 \sim 0.45$) between Ca and Mn in this interval is indicative of a possible secondary carbonate occurrence. Total Fe contents do not correlate with Ca and can thus point to the dominance of other Fe sources than ankerite. The characteristics in this interval are displayed equally by the MLC-XCS and by the conventionally measured samples. On the other hand, the upper two intervals with enrichments, situated in the upper Naaldwijk and upper Nieuwkoop Formations, at ~2 and ~1 m depth, respectively, are not well represented by the conventionally measured data. The first enrichment in the peat layer is depicted by high FeTR and TS and elevated trace metal contents. The trace metal abundance is also recorded by high Ni values. The FeTR and TS enrichments are less apparent in the conventionally measured samples. The second enrichment interval is situated in the uppermost part of the marine Naaldwijk Formation near the interface with the peat-bearing Nieuwkoop Formation. The clay sediments contain high amounts of FeTR, TS, Zn, As, Ni and Cr. There are very few to no reference data in this interval and thus the enrichment was not detected by the conventional methods. Sediments of the Nieuwkoop Formation commonly contain elevated contents of redox sensitive trace elements and high TS and FeTR contents, which is related to the organic-rich and sand-poor nature of the peat deposits (Dellwig et al., 2002; Bos et al., 2005). However, this is less common for the Naaldwijk Formation and the fact that the enrichment occurs just below the Nieuwkoop/Naaldwijk interface can be connected to influx of acid and/or DOC-rich pore water from the Nieuwkoop to the Naaldwijk sediments causing transfer of trace metals by paleohydrological leaching and immobilisation in the lower marine layer.

In the top 3–5 m of core B42E0748, the Naaldwijk Formation interchanges with the Nieuwkoop Formation (Fig. 8). Total S, FeTR, Ca-carbonate, As, Zn and Ni measured by XCS are high in the lower peat layer (4–4.5 m depth) and in the transition from the Naaldwijk Formation to the upper peat layer (~ 3.3 m depth; Fig. 8). Calcium carbonate, TS and FeTR of conventionally analysed samples do not clearly record these high contents. The median values for the Naaldwijk and Nieuwkoop Formations are 4.9% for calcium carbonate, 0.2% for FeTR and 0.1% for TS, which represent the baseline. Only a small increase in FeTR is seen in both layers of the Nieuwkoop Formation in the conventionally measured dataset. High As and Zn contents are also observed in the conventionally measured data but not in such detail. Particularly interesting are the enrichments of TS and FeTR in the sands of the Naaldwijk Formation, situated just below the peat layer, indicating a post-depositional diagenetic imprint. In core B43B0660 conventionally measured data generally records the element enrichments depicted by the XCS data (Fig. 2). However, the XCS data provides more detail, especially in intervals where sampling was sparse. Enrichment of FeTR, TS are not continuously recorded by conventional geochemical analyses

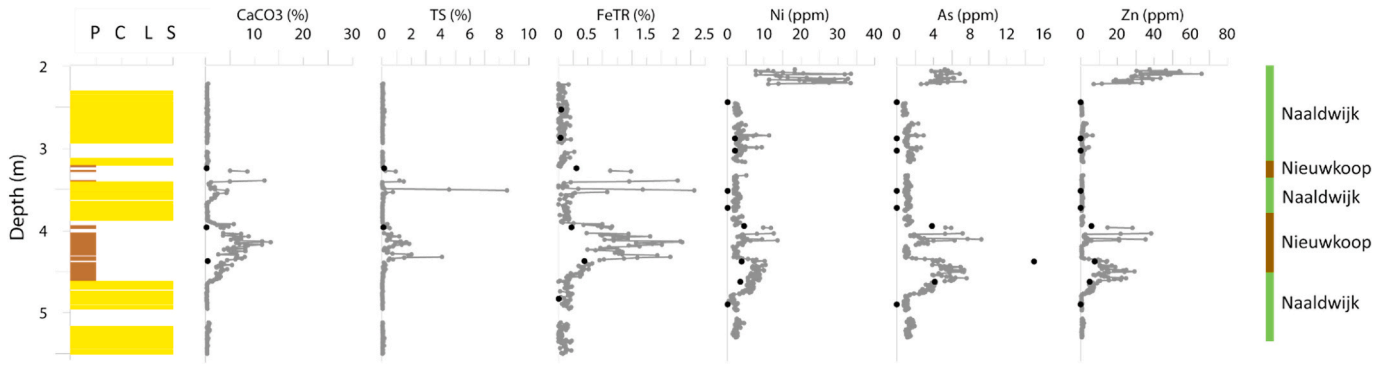

Fig. 8. Geochemical depth profiles for part of core B42E0748 with classification of lithology (P = peat, C = clay, L = loam, S = sand) and geological formation. The lines represent MLC-XCS data and the circles conventionally measured reference dataset.

in the loam dominated Waalre Formation (24–33 m depth) and in the Naaldwijk clays ~ 10.5 m depth (Fig. 2).

The results display that conventional element analyses capture many of the enrichment intervals but do not record small scale heterogeneities. The high-resolution XCS-MLC data has allowed a better and more detailed interpretation of geochemical signals compared to low-resolution conventional measurements for all cores.

5. Conclusions and recommendations

Time- and cost-effective geochemical characterisation of sediment is of general environmental interest. Continuous core scanning is therefore of high interest additionally or alternatively to classical, discrete sampling and conventional analysis. Conventionally measured element concentrations were compared to XCS-MLC data for environmental geochemical characterisation of sediments for four geologically heterogeneous sediment cores. A good correspondence was achieved between the conventionally measured and core-scanned data using a multivariate log-ratio calibration method for the elements Al, Ca, Cr, Fe, K, Sr, Mn, Ni, Pb, Rb, S, Si, Ti, Zn, Zr, and also for Br as proxy for organic matter. The correspondence between MLC-XCS and conventionally analysed samples was problematic for Cu, As and Ba, which is at least partially due to the low concentration ranges for these elements in the core material. The ranges in element contents were comparable for both approaches. An exception is the introduction of extreme values (more than twice the size of the conventionally measured value) for S, Fe, Ca and Zn. This may be due to an overestimation of high end values during log transformation, where high-end conventionally measured concentrations were lacking. In general, it is preferable for the calibration samples to overlap and the end members (low/high contents) to be sampled for the main elements of interest.

The good to moderate correlation enables application of chemometric methods to calculate parameters like Ca carbonate and reactive Fe. An obvious conclusion is that high-resolution core scanning provides a better understanding of the geochemical and mineralogical variability of sediment cores as well as information for the intervals where discrete samples have not been taken. Although both methods are capable of providing insights in average contents at the borehole scale, local features like diagenetic enrichments are not necessarily found by discrete sampling. We recommend that future XCS analyses should be preferably performed directly after core acquisition and before (discrete) sampling. Nevertheless, we have shown that valuable information can still be retrieved from MLC-XCS data from poorly stored core material. Considering the richness of core material stored in core repositories worldwide, interesting sections could be revisited for core-scanning to obtain high-resolution element archives.

Declaration of competing interest

The authors declare that they have no known competing financial interests or personal relationships that could have appeared to influence the work reported in this paper.

Acknowledgements

This research project was performed within the framework of the legal task assigned by the government to TNO to collect, to process and to make available geo-scientific data as well as information of the Dutch subsurface (funded by Ministry of the Interior and Kingdom Relations, PN 060.43296). This work at NIOZ was supported by the SCANALOGUE-project (ALWOP.2015.113) by the Netherlands Organization for Scientific Research (NWO), The Netherlands. This research was also partially funded by the NESSC Gravitation Grant (024.002.001) from the Dutch Ministry of Education, Culture and Science (OCW). R.H. would like to thank Rineke Gielens and Piet van Gaever for their help during the XRF-core-scan analyses. The authors thank three anonymous reviewers for their useful suggestions to improve the manuscript.

Appendix A. Supplementary data

Supplementary data to this article can be found online at https://doi.org/10.1016/j.apgeochem.2020.104824.

References

Acosta, J.A., Martinez-Martinez, S., Faz, A., Arocena, J., 2011. Accumulations of major and trace elements in particle size fractions of soils on eight different parent materials. Geoderma 161, 30–42.
Amorosi, A., Sammartino, I., Tateo, F., 2007. Evolution patterns of glaucony maturity: a mineralogical and geochemical approach. Deep Sea Res. II 54, 1364–1374.
Anawar, H.M., 2015. Sustainable rehabilitation of mining waste and acid mine drainage using geochemistry, mine type, mineralogy, texture, ore extraction and climate knowledge. J. Environ. Manag. 158, 111–121.
Bakker, I., Kiden, P., Schokker, J., Griffioen, J., 2007. De geotop van de ondergrond: een reactievat. Deelrapport 2. Eerste statistische karakterisatie van de geochemische reactiecapaciteit van het topsysteem in Noord-Brabant en het noorden van Limburg. TNO Bouw en Ondergrond report no. 2007-UR0324/A.
Bloemsma, M.R., 2015. Development of a Modelling Framework for Core Data Integration Using XRF Scanning. Ph.D. thesis. Delft University of Technology, The Netherlands, p. 229.
Boggs, S., 2009. Petrology of Sedimentary Rocks. Cambridge University Press, p. 600.
Bos, J.A.A., Huisman, D.J., Kiden, P., Hoek, W.Z., Van Geel, B., 2005. Early Holocene environmental change in the Kreekrak area (Zeeland, W-Netherlands): a multi-proxy analysis. Palaeogeogr. Palaeoclimatol. Palaeoecol. 227, 259–289, 2005.
Breeuwsma, A., 1990. Mineralogische samenstelling van de Nederlandse zand- en kleigronden. In: Locher, W.P., de Bakker, H. (Eds.), Bodemkunde Van Nederland. Deel 1 Algemene Bodemkunde. Malmberg, Den Bosch, pp. 103–107.
Cox, R., Lowe, D.R., Cullers, R.L., 1995. The influence of sediment recycling and basement composition on evolution of mudrock chemistry in the southwestern United States. Geochem. Cosmochim. Acta 59, 2919–2940.
Croudace, I.W., Rindby, A., Rothwell, R.G., 2006. ITRAX: description and evaluation of a new multifunction. X-ray core scanner. In: Rothwell, R.G. (Ed.), New Techniques in

Sediment Core Analysis, vol. 267. Geological Society, London, pp. 51–63. Special Publication.
Croudace, I.W., Rothwell, R.G., 2015. Micro-XRF Studies of Sediment Cores: Applications of a Non-destructive Tool for the Environmental Sciences. Springer Science+ Business Media, Dordrecht.
Davide, V., Pardos, M., Diserens, J., Ugazio, G., Thomas, R., Dominik, J., 2003. Characterisation of bed sediments and suspension of the river po (Italy) during normal and high flow velocities. Water Res. 37, 2847–2864.
De Gans, W., 2007. Quaternary geology. In: Wong, ThE., Batjes, D.A.J., de Jager, J. (Eds.), Geology of the Netherlands. Royal Neth. Acad. Arts Sci., pp. 173–195
Dellwig, O., Böttcher, M.E., Lipinski, M., Brumsack, H.J., 2002. Trace metals in Holocene coastal peats and their relation to pyrite formation (NW Germany). Chem. Geol. 182, 423–442.
Dellwig, O., Watermann, F., Brumsack, H.-J., Gerdes, G., 1999. High-resolution reconstruction of a Holocene coastal sequence (NW Germany) using inorganic-geochemical data and diatom inventories. Estuar. Coast Shelf Sci. 48, 617–633.
Dellwig, O., Watermann, F., Brumsack, H.-J., Gerdes, G., Krumbein, W.E., 2001. Sulphur and iron geochemistry of Holocene coastal peats ŽNW Germany: a tool for palaeoenvironmental reconstruction. Palaeogeogr. Palaeoclimatol. Palaeoecol. 167, 359–379.
Doulati Ardejani, F., Jodieri Shokri, B., Moradzadeh, A., Shafaei, S.Z., Kakaei, R., 2011. Geochemical characterisation of pyrite oxidation and environmental problems related to release and transport of metals from a coal washing low-grade waste dump, Shahrood, northeast Iran. Environ. Monit. Assess. 183, 41–55.
Falster, G., Tyler, J., Grant, K.M., Tibby, J., Turney, C., Löhr, S., Jacobsen, G., Kershaw, A.P., 2018. Millennial-scale variability in south-east Australasian hydroclimate between 30,000 and 10,000 years ago. Quat. Sci. Rev. 192, 106–122.
Grant, K.M., Rohling, E.J., Westerhold, T., Zabel, M., Heslop, D., Konijnendijk, T., Lourens, L.J., 2017. A 3 million year index for North African humidity/aridity and the implication of potential pan-African Humid periods. Quat. Sci. Rev. 171, 100–118.
Gregory, B.R.B., Patterson, R.T., Reinhardt, E.G., Galloway, J.M., 2019. The iBox-FC: a new containment vessel for Itrax X-ray fluorescence core-scanning of freeze cores. Quat. Int. 514, 76–84.
Griffioen, J., Appelo, C.A.J., 1993. Nature and extent of carbonate precipitation during aquifer thermal energy storage. Appl. Geochem. 8, 161–176.
Griffioen, J., Klaver, G., Westerhoff, W.E., 2016. The mineralogy of suspended matter, fresh and Cenozoic sediments in the fluvio-deltaic Rhine–Meuse–Scheldt–Ems area, The Netherlands: an overview and review. Neth. J. Geosci. 95, 23–107.
Griffioen, J., Klein, J., Van Gaans, P.F.M., 2012. Reaction capacity characterisation of shallow sedimentary deposits in geologically different regions of The Netherlands. J. Contam. Hydrol. 127, 30–46.
Heerdink, R., Griffioen, J., 2008. Methodeontwikkeling voor het berekenen van het gehalte reactief ijzer uit totaalgehaltes ijzer en aluminium in sediment. TNO report, 2008-U-R1278/A.
Hennekam, R., Sweere, T., Tjallingii, R., de Lange, G.J., Reichart, G.-J., 2019. Trace metal analysis of sediment cores using a novel X-ray fluorescence core scanning method. Quat. Int. 514, 55–67.
Huisman, D.J., Kiden, P., 1998. A geochemical record of Late Cenozoic sedimentation history in the southern Netherlands. Geol. Mijnbouw 76, 277–292.
Jansen, J.H.F., Van der Gaast, S.J., Koster, B., Vaars, A.J., 1998. CORTEX, a shipboard XRF-scanner for element analyses in split sediment cores. Mar. Geol. 151, 143–153.
Klein, J., Griffioen, J., 2010. Organisch materiaal, kalk en zwavel in sediment: uitwerking van analyses naar gehaltes. TNO Bouw en Ondergrond, rapport. TNO-034-UT-2010-02327/A.
Koelmans, A.A., 1998. Geochemistry of suspended and settling solids in two freshwater lakes. Hydrobiologia 364, 15–29.
Lee, A.S., Huang, J.J.S., Burr, G., Kao, L.C., Wei, K.Y., Liou, S.Y.H., 2019. High resolution record of heavy metals from estuary sediments of Nankan River (Taiwan) assessed by rigorous multivariate statistical analysis. Quat. Int. 527, 44–51.
Odin, G.S., Matter, A., 1981. De glauconiarum origine. J. Sediment. Petrol. 28, 611–641.
Pedersen, K.B., Kirkelund, G.M., Ottosen, L.M., Jensen, P.E., Lejon, T., 2015. Multivariate methods for evaluating the efficiency of electrodialytic removal of heavy metals from polluted harbour sediments. J. Hazard Mater. 283, 712–720.
Pit, I.R., Griffioen, J., Wassen, M.J., 2017. Environmental geochemistry of a mega beach nourishment in The Netherlands: monitoring freshening and oxidation processes. Appl. Geochem. 80, 72–89.
Poulton, S.W., Raiswell, R., 2002. Chemical and physical characteristics of iron oxides in riverine and glacial meltwater sediments. Chem. Geol. 218 (3–4), 203–221.
Postma, D., 1982. Pyrite and siderite formation in brackish and fresh water swamp sediments. Am. J. Sci. (282), 1151–1183.
Prommer, H., Stuyfzand, P.J., 2005. Identification of temperature-dependent water quality changes during a deep well injection experiment in a pyritic aquifer. Environ. Sci. Technol. 39, 2200–2209.
Reimann, C., Fabian, K., Birke, M., Filzmoser, P., Demetriades, A., Negrel, P., Oorts, K., Matschullat, J., de Caritat, P., The GEMAS Project Team, 2018. GEMAS: establishing geochemical background and threshold for 53 chemical elements in European agricultural soil. Appl. Geochem. 8 (B), 302–318.
Reimann, C., Garrett, R.G.(, 2005. Geochemical background - concept and reality. Sci. Total Environ. 350 (1–3), 12–27.
Richter, T.O., van der Gaast, S., Koster, B., Vaars, A., Gieles, R., de Stigter, H.C., de Haas, H., van Weering, T.C.E., 2006. The Avaatech XRF Core Scanner: technical description and applications to NE Atlantic sediments. In: Rothwell, R.G. (Ed.), New Techniques in Sediment Core Analysis. Special Publications. Geological Society, London, pp. 39–50.
Rodrigues, S.M., Henriques, B., da Silva, E.F., Pereira, M.E., Duarte, A.C., Römkens, P.F. A.M., 2010. Evaluation of an approach for the characterization of reactive and available pools of twenty potentially toxic elements in soils: Part I - the role of key soil properties in the variation of contaminants' reactivity. Chemosphere 81, 1549–1559.
Saaltink, R., Griffioen, J., Mol, G., Birke, M., Mann, A., GEMAS-projectteam, 2014. Geogenic and agricultural controls on the geochemical composition of European agricultural soils. J. Soils Sediments 14, 121–137.
Saaltink, R., Dekker, S.C., Griffioen, J., Wassen, M.J., 2016. Wetland eco-engineering: measuring and modeling feedbacks of oxidation processes between plants and clay-rich material. Biogeosciences 13, 4945–4957.
Salonen, V.P., Korkka-Niemi, K., 2007. Influence of parent sediments on the concentration of heavy metals in urban and suburban soils in Turku, Finland. Appl. Geochem. 22, 906–918.
Singh, K.P., Malik, A., Basant, A., Ojha, P., 2008. Vertical characterization of soil contamination using multi-way modeling - a case study. Environ. Monit. Assess. 146, 19–32.
Sterckemann, T., Douay, F., Baize, D., Fourrier, H., Proix, N., Schvartz, C., 2004. Factors affecting trace element concentrations in soils developed on recent marine deposits from northern France. Appl. Geochem. 19, 89–103.
Tebbens, L.A., Veldkamp, A., Kroonenberg, S.B., 2000. Natural Compositional Variation of the River Meuse (Maas) Suspended Load: a 13 Ka Bulk Geochemical Record from the Upper Kreftenheije and Betuwe Formations in Northern Limburg. Netherlands Journal of Geosciences, vol. 79, pp. 391–409.
Tjallingii, R., Röhl, U., Kölling, M., Bickert, T., 2007. Influence of the water content on X-ray fluorescence core-scanning measurements in soft marine sediments. G-cubed 8, Q02004.
Van de Veer, G., 2006. Geochemical Soil Survey of the Netherlands - Atlas of Major and Trace Elements in Topsoil and Parent Material; Assessment of Natural and Anthropogenic Enrichment Factors. PhD Thesis. Utrecht University, The Netherlamnds.
Van Gaans, P.F.M., Spijker, J., Vriend, S.P., De Jong, N., 2007. Patterns in soil quality: natural geochemical variability versus anthropogenic impact in soils of Zeeland, The Netherlands. Int. J. Geographical Information Sci. 21, 569–587.
Van Gaans, P.F.M., Griffioen, J., Mol, G., Klaver, G., 2011. Geochemical reactivity of subsurface sediments as potential buffer to anthropogenic inputs: a strategy for regional characterization in The Netherlands. J. Soils Sediments 11, 336–351.
Von Eynatten, H., Barcelo-Vidal, C., Pawlowsky-Glahn, V., 2003. Composition and discrimination of sandstones: a statistical evaluation of different analytical methods. J. Sediment. Res. 73, 47–57.
Wanner, C., Eggenberger, U., Mäder, U., 2012. A chromate-contaminated site in southern Switzerland - Part 2: reactive transport modeling to optimize remediation options. Appl. Geochem. 27, 655–662.
Weltje, G.J., Tjallingii, R., 2008. Calibration of XRF core scanners for quantitative geochemical logging of sediment cores: theory and application. Earth Planet Sci. Lett. 274, 423–438.
Weltje, G.J., Bloemsma, M., Tjallingii, R., Heslop, D., Röhl, U., Croudace, I.W., 2015. Prediction of geochemical composition from XRF core scanner data: a new multivariate approach including automatic selection of calibration samples and quantification of uncertainties. In: Croudace, I.W., Rothwell, R.G. (Eds.), Micro-XRF Studies of Sediment Cores. Springer Science+Business Media, Dordrecht, pp. 507–534.
Yamasaki, S., Takeda, A., Kimura, K., Tsuchiya, N., 2016. Underestimation of chromium and zirconium in soils by hydrofluoric acid digestion and inductively coupled plasma-mass spectrometry. Soil Sci. Plant Nutr. 62 (No. 2), 121–126.
Yan, X.-P., Kerrich, R., Hendry, M.J., 2009. Trace element geochemistry of a thick till and clay-rich aquitard sequence, Saskatchewan, Canada. Chem. Geol. 164, 93–120.
Ziegler, M., Jilbert, T., De Lange, G.J., Lourens, L.J., Reichart, G.-J., 2008. Bromine counts from XRF scanning as an estimate of the marine organic carbon content of sediment cores. G-cubed 9, Q05009.